JOURNAL OF SPACECRAFT AND ROCKETS
Vol. 47, No. 1, January–February 2010

Improvements to Power-On Base Pressure Prediction for the Aeroprediction Code

F. G. Moore and L. Y. Moore
Aeroprediction, Inc., King George, Virginia 22485-7076

DOI: 10.2514/1.45602

New technology has been developed and added to the power-on base drag prediction model in the aeroprediction code. The new technology showed improvement over the January 2009 release of the code compared with experiment for all cases considered. Of particular note is the capability to predict base pressure for power-off conditions and at all values of power-on including base bleed and values of thrust coefficient below where the minimum value of power-on base pressure occurs. To the authors' knowledge, this is the first theoretical method available to predict power-on base pressure at any value of thrust coefficient.

Nomenclature

A_r	=	reference area which is cross-sectional area of body, ft^2
A_t	=	area of rocket motor nozzle throat cross section, ft^2
C_{P_B}	=	base pressure coefficient
C_T	=	thrust coefficient, thrust/$(\frac{1}{2}\rho_\infty V_\infty^2 A_{\text{ref}})$
d	=	diameter
d_B	=	diameter at the base, ft
d_j	=	diameter of the jet exit, ft
d_r	=	body reference diameter, ft
I	=	nondimensional base bleed injection parameter
M	=	Mach number
$\dot{m}$	=	mass rate of flow, ρAV
P	=	static pressure, lb/ft^2
T	=	temperature, °R, or thrust, lbs
V	=	velocity, ft/s
x_j	=	distance of jet exit from body base (positive behind base)
α	=	angle of attack, deg
β	=	parameter used in base bleed methodology
γ	=	ratio of specific heats
θ_j	=	nozzle exit angle
ρ	=	density, slugs/ft^3
σ	=	parameter used in base bleed methodology

Subscripts

B	=	conditions at base of body
C	=	conditions in rocket motor chamber
j	=	conditions at jet exit
r	=	reference conditions
t	=	conditions at nozzle throat
∞	=	freestream conditions

Superscript

*	=	conditions at which $M = 1.0$

Received 22 May 2009; revision received 10 August 2009; accepted for publication 11 September 2009.

*President, 9449 Grover Drive; drfgmoore@hotmail.com. Associate Fellow AIAA.
†Computer Scientist, 9449 Grover Drive.

Introduction

THE aeroprediction code (APC) is a semi-empirical code that computes aerodynamics rapidly on most weapon configurations with good accuracy and over a broad class of flight conditions. The code uses analytical methods at low angles of attack and empirical methods derived from several large wind-tunnel databases at high angles of attack to obtain good accuracy. Ten versions of the code have been produced over a 37-year span, the latest version being the 2009 version of the APC (AP09). Each version has added new technology relevant to meeting the requirements of the weapons technical community.

Several years ago, Aeroprediction, Inc. (API) had a small consulting contract with a long-time user of the aeroprediction code to look at answers obtained from the 2005 version of the aeroprediction code (AP05) for power-on base drag at transonic Mach numbers. After looking into the problem, it was concluded that the AP05 computations were being done for low values of thrust coefficient and at low Mach numbers at which the power-on base drag methodology was not very accurate. In addition, at very low values of thrust or jet momentum flux ratio, the base pressure reaches a minimum value and then increases from the minimum as C_T is decreased further. Neither the AP05 [1] or AP09 [2] can account for the minimum value of base pressure at low values of thrust coefficient or jet momentum flux ratio. Thrust coefficient and jet momentum flux ratio (RMF) are closely related through the following equation:

$$C_T = 2\text{RMF} + \left(\frac{d_j}{d_r}\right)^2 \frac{2}{\gamma_\infty M_\infty^2}\left(\frac{P_j}{P_\infty} - 1\right) \tag{1}$$

Figure 1 illustrates typical base pressure [3,4] as a function of RMF or C_T for power off (RMF = 0), base bleed (region AB of Fig. 1), and larger values of RMF (region CD of Fig. 1). Figure 1 shows two curves illustrating the effect of freestream Mach number as well as RMF or C_T on P_B/P_∞. Examining one of the curves in Fig. 1, it is seen that, at RMF = 0, we have the values of power-off base drag. Initially, at low values of power on, referred to as base bleed, P_B/P_∞ increases up to a maximum (point B) at a low value of RMF, thus decreasing base drag. As RMF is increased, P_B/P_∞ decreases to a minimum (where base drag is a maximum) at point C. As RMF is increased beyond point C, P_B/P_∞ begins increasing again and, at large values of RMF, can actually be positive (a base thrust versus a base drag).

The AP05 (or AP09) computes base pressure in the base bleed region AB and the larger values of RMF region CD of Fig. 1. In region AB, the APC uses a modified version of Danberg's method [5,6] and, in region CD, the APC uses a modified version of Brazzel and Henderson's method [5,7]. Unfortunately, the APC does not predict the value of point C in Fig. 1. Thus, for values of RMF between points B and C on Fig. 1, the APC will simply provide values of P_B/P_∞ along the curve between C and D, giving much lower

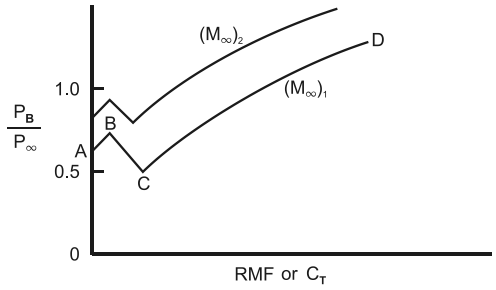

Point	Definition
A	Power-off base pressure
B	Upper value of (P_B/P_∞) due to base bleed
C	Minimum value of (P_B/P_∞) from power on
D	Value of (P_B/P_∞) for a typical large value of RMF

Fig. 1 Generic representation of base pressure as a function RMF or C_T for a given freestream Mach number.

values of P_B/P_∞ than data would suggest (and, hence, much higher base drag). The improved base drag methodology of [5] clearly states the fact that the APC is not applicable in region BC of Fig. 1; however, without the definition of point C, the unsuspecting user will get erroneous values of P_B/P_∞ from the AP05 or AP09 for region BC in Fig. 1 without knowing the values are incorrect.

The purpose of this paper is to define the technology to allow power-on base drag to be computed for all values of RMF in the AP09 [2]. This new technology will be included in the January 2010 release of the AP09, referred to as the AP09/10.

In addition to approximating the minimum base pressure point C in Fig. 1, it was found that improvements in accuracy of the power-on base drag methodology of [5] could be made. Thus the goal of the present effort is to improve the accuracy of the power-on base drag methodology over a wide range of thrust or mass flow ratio values, while allowing power-on base pressure to be computed at all values of RMF or C_T.

History of Base Drag Computations in the Aeroprediction Code

The power-off and -on base drag methodology of the AP09 has been developed over a period of nearly 40 years. A brief history of the development of the base drag methodology will be given, along with references. The current AP09 base drag methodology will then be summarized. However, the reader will be referred to the references for the derivation of the theory, as it will not be repeated here.

The power-off base drag methodology will be summarized first. The first three versions of the APC, the AP72 [8], AP74 [9], and AP77 [10], had power-off base drag only. The power-off base drag was for axisymmetric bodies only (3-D base pressure) in the AP72 and was extended to the region behind blunt trailing-edge fins (2-D base pressure) in the AP74. The power-off base drag was based on an average of 3-D [8] and 2-D [9] base pressure databases found in the literature at that time. Corrections for boat tails, flares, fin thickness, and fin location were accounted for. However, the effect of fins on base pressure databases was very limited.

The power-off base drag prediction methodology was improved in the AP93 [11] based on a new wind-tunnel database [12]. The new wind-tunnel database made slight improvements to the body-alone base drag prediction and made more significant improvements for the effect of fin location, fin thickness, fin control deflection, and body angle of attack. The final improvement in the power-off base drag was to improve the base pressure prediction for configurations with flares and to make some adjustments to the 2-D base pressure coefficient at sub- and transonic speeds. These modifications were added to the AP02 [4].

The initial approach to predict the effect of the engine on base pressure was integrated into the APC in the late 1970s. The method was an extension of the Brazzel method [5,7]. The Brazzel method [7] was limited to RMF values of about 2.5 or less. Moore and Hymer [5] formally summarized and documented the modifications to the Brazzel method [7] for higher values of RMF. Moore and Hymer [5] also documented several other extensions to the Brazzel method that allowed the user to input different engine parameters than P_C/P_∞ if P_C/P_∞ were not readily available.

The Brazzel method was also limited to values of RMF above the point at which P_B/P_∞ reached a minimum (point C of Fig. 1). As a result of this limitation, a modified version of Danberg's method [5,6] was integrated into the AP02 [5] to compute base bleed effects on base drag in region AN of Fig. 1.

The general approach to compute base drag using the AP09 [2] is as follows:

1) Compute power-off, body-alone, base pressure for straight afterbody.

2) If base bleed, compute modified value of base pressure using modified Danberg method.

3) If power on, determine value of base pressure using either Brazzel, modified Brazzel, or conceptual design alternative.

4) Compute body-alone AOA effects.

5) Compute modifications to body-alone base drag due to tail fins (includes effects of fin deflection and angle of attack, fin thickness, and fin location with respect to body alone).

6) Compute effect of boat tail or flare on base drag if either is present.

As already mentioned, the AP09 methodology is not applicable to region BC of Fig. 1. The next section of this paper will define the methodology to allow base drag prediction in region BC as well as the modifications of the methodology in [2] needed to improve the overall power-on base drag prediction accuracy.

Analysis

As mentioned in the Introduction, our goal is to improve the overall accuracy of the power-on base drag prediction methodology used in [2] as well as to define P_B/P_∞ for all values of power on, including region BC of Fig. 1. Therefore, we will deal first of all with the accuracy improvements made to the methodology in [2] and then define the approach to predict base pressure of region BC in Fig. 1.

Refinements to Improve Power-On Prediction of P_B/P_∞

The present mathematical model for power-on base drag used in [2,5] is defined by the following equations, with Fig. 2 illustrating much of the nomenclature for the power-on and base bleed engine concepts.

1) Base bleed (inputs: I, T_j)

$$P_B/P_\infty = \frac{\gamma_\infty M_\infty^2}{2}(C_{P_B})_{\mathrm{NF},\alpha=0} + 1 + \frac{\sigma I}{1+2.6\sigma I} \tag{2}$$

$$(C_{P_B})_{\mathrm{NF},\alpha=0} = \frac{2}{\gamma M_\infty^2}\left[\frac{P_B}{P_\infty} - 1\right] \tag{3}$$

2) Power on: Brazzel (inputs: P_C/P_∞, A_T/A_j, x_j/d_r, γ_j)

a)

$$P_B/P_\infty = \frac{T_j}{T_j^*}\left[0.19 + 1.28\left(\frac{\mathrm{RMF}}{1+\mathrm{RMF}}\right)\right]\left[\frac{3.5}{1+2.5(d_B/d_r)^2}\right] + 0.047(5-M_\infty)[2(x_j/d_B) + (x_j/d_B)^2] \tag{4}$$

b) Compute C_{P_B} from Eq. (3).

3) Power on: modified Brazzel (inputs: thrust, d_j/d_r, γ_j, x_j/d_r, and either P_C/P_∞, P_j/P_∞ or M_j)

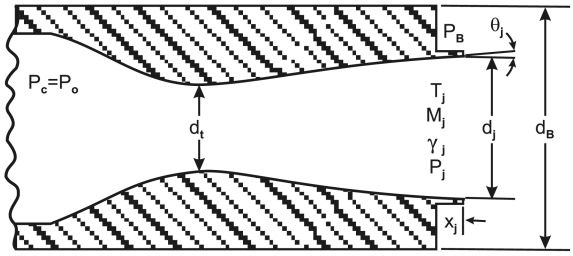

a) Rocket engine parameters

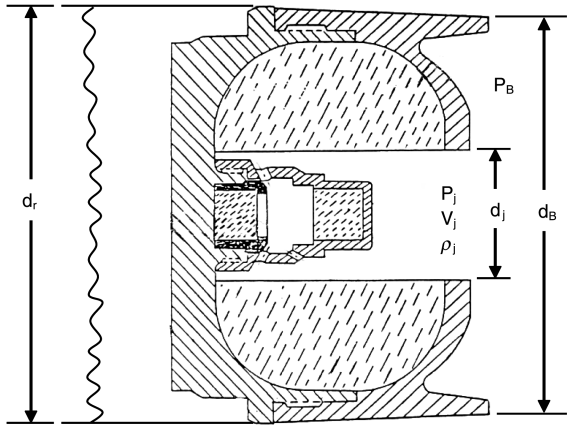

b) Typical projectile base bleed configuration [6]

Fig. 2 Nomenclature for power-on conditions for rockets and base bleed concepts.

a)

$$P_B/P_\infty = \left(\frac{T_j}{T_j^*}\right)^N \left[C_1(C_T, M_\infty) + C_2(C_T, M_\infty)\left(\frac{\text{RMF}}{1+\text{RMF}}\right)\right] \times f(d_B/d_r) + 0.047(5 - M_\infty)[2(x_j/d_B) + (x_j/d_B)^2];$$
$$f(d_B/d_r)\text{defined by Eqs. 4–7 of text} \tag{5}$$

b) Compute C_{P_B} from Eq. (3)

4) Power on: conceptual design

$$C_{A_B} = f[(C_{A_B})_{\text{power off}}]; \qquad f = -1.5 \quad \text{to } 2.5 \tag{6}$$

In referring to Eqs. (2–6), the user of the AP09 has the option of requesting base bleed (region AB of Fig. 1) or power on (region CD of Fig. 1) with the options of Brazzel, modified Brazzel or conceptual design. Also note that Eq. (5) is similar to Eq. (4) except the coefficients C_1 and C_2, which are constant in Eq. (4), are functions of C_T and M_∞ in Eq. (5). Equation (2) for base bleed is relevant to Fig. 2b, whereas Eqs. (4–6) are relevant to Fig. 2a. C_1 and C_2 of Eqs. (2–6) are defined by Table 1. $f(d_B/d_r)$, T_j/T_j^*, and N of Eqs. (2–6) are defined by the following four equations:

Table 1 Empirical parameters to define power-on base pressure [5]

	$C_1\ (C_T, M_\infty)$					$C_2\ (M_\infty, C_T)$	
	C_T					C_T	
M_∞	≤ 1.0	2.0	20	40	≥ 70	≤ 1.0	≥ 2.0
≤ 0.9	0.19	0.16	−0.06	0.02	0.0	1.24	1.24
1.0	0.19	−0.085	−0.06	0.02	0.0	1.28	1.37
1.25	0.19	−0.085	−0.01	0.02	0.0	1.28	1.47
1.65	0.19	−0.175	−0.06	0.04	0.0	1.28	1.70
2.0	0.19	−0.30	−0.20	0.02	0.0	1.28	1.90
2.5	0.19	−0.45	−0.23	0.01	0.0	1.28	2.30
3.0	0.19	−0.55	−0.22	−0.03	0.0	1.28	2.50
≥ 4.0	0.19	−0.65	−0.10	−0.04	0.0	1.28	2.7

$$P_B/P_\infty = \left(\frac{T_j}{T_j^*}\right)^N \left[C_1(C_T, M_\infty) + C_2\left(\frac{\text{RMF}}{1+\text{RMF}}\right)\right] f(d_B/d_r) + f(x_j/d) \tag{7}$$

where

$$N = \frac{12 - C_T}{11}, \qquad 1.0 \le C_T < 12 = 0, \qquad C_T \ge 12.0; \tag{8}$$
$$C_1(C_T, M_\infty) \quad \text{and} \quad C_2(M_\infty, C_T) \text{ from Table 1}$$

$$(T_j/T_j^*)_{\min} = 0.7 - (M_\infty - 1.2)\left(\frac{0.7 - T_j/T_j^*}{0.3}\right);$$
$$1.2 \le M_\infty \le 1.5 = 0.7; \qquad M_\infty < 1.2 \tag{9}$$
$$(T_j/T_j^*)_{\min} = \frac{\frac{\gamma_j+1}{2}}{1 + \frac{\gamma_j - 1}{2} M_j^2}; \qquad M_\infty > 1.5$$

$$\text{If } d_B/d_r < 1.0 \qquad f(d_B/d_r) = \frac{3.5}{1 + 2.5(d_B/d_r)^2};$$
$$C_T \le 6.0 = 1 + \frac{12 - C_T}{6}\left[\frac{3.5}{1 + 2.5(d_B/d_r)^2} - 1\right];$$
$$6 \le C_T \le 12 = 1; \qquad C_T > 12.0 \qquad \text{If } d_B/d_r > 1.0 \tag{10}$$
$$f(d_B/d_r) = \frac{3.5}{1 + 2.5(d_B/d_r)^2};$$
$$C_T \le 25.0 = 1 + \frac{75 - C_T}{50}\left[\frac{3.5}{1 + 2.5(d_B/d_r)^2} - 1\right];$$
$$25 \le C_T \le 75 = 1; \qquad C_T > 75$$

The goal here is to modify Table 1 to allow a more accurate prediction of P_B/P_∞ of region CD in Fig. 1. The approach to accomplish this goal is as follows:

1) Refine C_1 and C_2 at $M_j = 1.0$ (so that $T_j/T_j^* = 1.0$) for a cylindrical afterbody ($f(d_B/d_r) = 1$).

2) Refine N (exponent for T_j/T_j^*) when $M_j \ne 1.0$ for a cylindrical afterbody ($f(d_B/d_r) = 1$).

3) Refine $f(d_B/d_r)$ for both a boat-tail and a flare case when $M_j = 1.0$ and then when $M_j \ne 1.0$.

The refinements will be done based on comparisons with the data, most of which are cold-flow wind-tunnel data. Although most of the data used for comparison purposes is cold flow, in principle, effects of a hot gas are partially accounted for by the parameters T_j/T_j^* and γ, both of which vary as gas temperature rises. No account of chemical reactions from propellants in the base region is made with the current methodology. The data used for refining the constants C_1 (C_T, M_∞) and C_2 (C_T, M_∞) were primarily from Deep et al. [13]. Using [13], an expanded table of C_1 and C_2 was developed and given here as Table 2. In comparing Table 2 with Table 1, it is seen that Table 2 expanded the range of C_1 from five to seven values of thrust coefficient, modified the values of Mach numbers used slightly, and changed the values of C_1 and C_2 slightly due to expanding the number of values of C_T used.

Figure 3 compares the use of Table 2 (AP09/10) for estimating the coefficients of C_1 and C_2 with the Table 1 values used in the AP09/09 and the constant values of $C_1 = 0.19$ and $C_2 = 1.28$ used by Brazzel and Henderson [7] with the experimental data of Deep et al. [13]. In examining Fig. 3, it is seen that the modified method of Brazzel and Henderson used in the AP09/09 is superior in general to the Brazzel method. More important, the AP09/10, which uses the constants in Table 2, almost duplicates the experimental data (because the data was used to help generate the new constants C_1 and C_2) and is clearly superior to the modified Brazzel and Brazzel methods, both of which are used in the AP09/09. The standard Brazzel method will remain in the AP09/10, but the modified Brazzel method will be initially

Table 2 Improved empirical parameters for modified Brazzel method

M_∞	C_1 (C_T, M_∞)							C_2 (M_∞, C_T)	
	C_T							C_T	
	≤ 1.0	1.5	2.0	5.0	15.0	30.0	≥ 50.0	≤ 1.0	≥ 2.0
≤ 0.9	0.19	0.23	.28	0.06	0.04	0.07	0.07	1.28	1.28
1.0	0.19	0.13	0.07	0.03	0.17	0.20	0.20	0.28	1.28
1.2	0.19	0.13	0.13	.08	0.29	0.27	0.22	1.28	1.35
1.5	0.19	0.10	0.07	0	0.14	0.21	0.19	1.28	1.60
2.0	0.19	0.08	0.04	−0.01	0.20	0.38	0.41	1.28	1.70
2.5	0.19	0.10	0	−0.06	0.26	0.55	0.60	1.28	1.80
3.0	0.19	0.08	−0.05	−0.25	0.13	0.60	0.65	1.28	2.10
≥ 4.0	0.19	0.07	−0.10	−0.25	0.15	0.62	0.65	1.28	2.20

improved by replacing Table 1 with Table 2 in the power-on base drag computations.

The next area investigated for improving the power-on base drag prediction model is the term $(T_j/T_j^*)^N$ in Eq. (8). Brazzel and Henderson [7] used this term, which defines the jet exit temperature at some exit Mach number to the jet temperature at an exit Mach number of 1, to account for the jet exit Mach number. Brazzel's method [7] used (T_j/T_j^*) directly, where $N = 1$ and there were no limitations on (T_j/T_j^*), as shown in Eq. (8) for the modified Brazzel method. In using the new Table 2 coefficients on a broader class of configurations than originally investigated for the improved power-on model of the AP02 [5] (known as the modified Brazzel method and shown as AP09/09 in Fig. 3), it was found several changes were needed compared with the definition in Eqs. (8) and (9) of N and (T_j/T_j^*) limitations. First of all, the value of N goes to a minimum value of 0.1 for values of C_T greater than 30 versus 0 for values of C_T

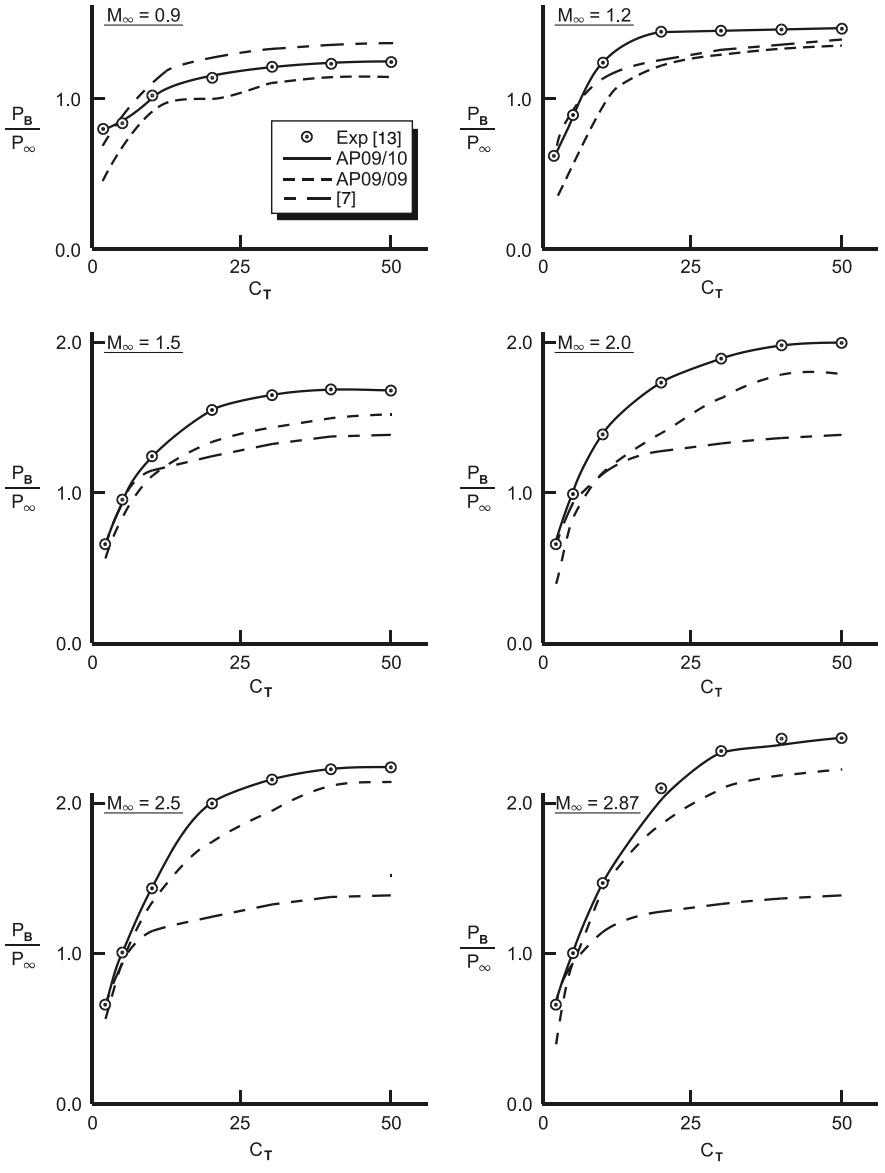

Fig. 3 Comparison of theory to experiment for power-on base pressure ($d_j/d_r = 0.45$, $d_B/d_r = 1.0$, $M_j = 1.0$).

greater than 12. Second, $(T_j/T_j^*)_{\min}$ in Eq. (9) is a function of freestream Mach number only, whereas for the AP09/10 it is still a function of Mach number, but with different limitations.

The specific equations that govern N and $(T_j/T_j^*)_{\min}$ in Eqs. (8) and (9) are

$$N = 1.031 - .031C_T, \quad 1 \leq C_T \leq 30 = 0.1, \quad C_T > 30 = 1, \quad C_T \leq 1 \tag{11}$$

$$\left(\frac{T_j}{T_j^*}\right)_{\min} = \frac{T_j}{T_j^*} = \frac{\frac{\gamma_j+1}{2}}{1+(\frac{\gamma_j-1}{2})M_j^2}; \quad M_\infty \geq 2.0$$

$$\left(\frac{T_j}{T_j^*}\right)_{\min} = 0.7 - \frac{(M_\infty - 1.2)}{0.8}[0.7 - (T_j/T_j^*)]; \quad 1.2 \leq M_\infty < 2.0$$

$$= 0.82 - 0.1M_\infty; \quad M_\infty < 1.2 \tag{12}$$

Figure 4 compares the AP09/10, AP09/09 and Brazzel methods with the experimental data [14]. Henderson's data [14] used several nozzles with jet exit Mach numbers ranging from 1.7 to 2.7 and nozzle exit angles from 9.1 to 23.3 deg. Mach numbers ranged from 0.9 to 2.5. Figure 4 shows that the AP09/10 improves the prediction of P_B/P_∞ for low thrust coefficient values over the AP09/09, but results are mixed at higher values of C_T. Both AP09/10 and AP09/09 compare very well with the experimental data. The Brazzel method [7] does not compare well with the data due to using constant values of $C_1 = 0.19$ and $C_2 = 1.28$ (see Table 2) and allowing (T_j/T_j^*) to have its full value independent of thrust coefficient.

The final area to refine is the term $f(d_B/d_r)$ in Eq. (10) for boat tails and flares. Brazzel and Henderson [7] define $f(d_B/d_r)$ as

$$f(d_B/d_r) = \frac{3.5}{1 + 2.5(d_B/d_r)^2} \tag{13}$$

for all boat tails or flares independent of thrust coefficient or other constraints. Several modifications to the AP09/09 formulation of Eq. (10) for $f(d_B/d_r)$ were made, particularly for low thrust levels. One reason the AP09/09 put a limit of a minimum value of $C_T = 1.0$ for its calculations was the poor accuracy for boat-tail cases. For boat tails, a complex limit was placed on $f(d_B/d_r)$. The limit was a function of Mach number and thrust coefficient. Also, for low thrust levels $f(d_B/d_r)$ was increased. The following changes were the final modifications to $f(d_B/d_r)$ for boat tails. These changes were arrived at based on a more exhaustive comparison with the experimental data than was previously done. For very low C_T,

$$f(d_B/d_r)_1 = \left[\frac{3.5}{1 + 2.5(d_B/d_r)^2}\right]^M \tag{14}$$

where $M = 1$ for $C_T \geq 1.5$, $M = 1.5$ for $C_T \leq 0.5$, $M = (3.5 - C_T)/2$ for $0.5 < C_T < 1.5$.

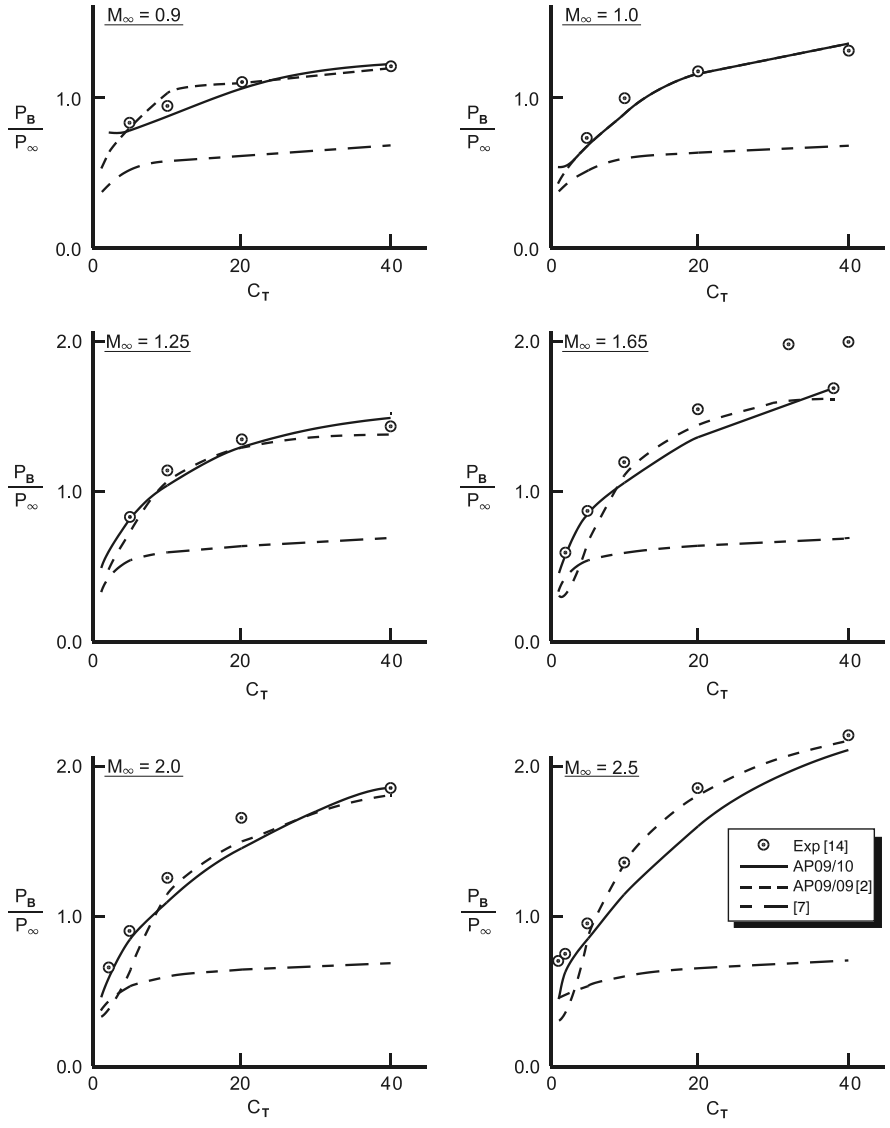

Fig. 4 Comparison of theory and experiment for power-on base drag ($d_j/d_r = 0.8, d_B/d_r = 1.0, M_j = 1.7$–$2.7$).

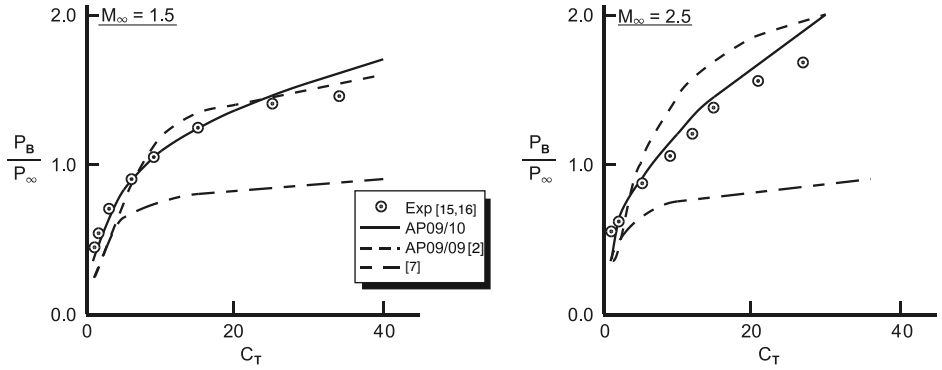

Fig. 5 Comparison of theory and experiment for power-on base pressure ($d_j/d_r = 0.45$, $d_B/d_r = 0.86$, $M_j = 2.7$).

For values of $C_T > 1.5$, a more complicated expression was derived:

$$f(d_B/d_r) = 1 + [(C_T)_{\max} - C_T][f(d_B/d_r)_1 - 1][(C_T)_{\max} - 2] \tag{15}$$

where $(C_T)_{\max} = 40$, $M_\infty \le 0.7$; $(C_T)_{\max} = 25$, $M_\infty \ge 1.5$; $(C_T)_{\max} = 53.125 - 18.75M_\infty$, $0.7 < M_\infty < 1.5$.

Figure 5 compares the new AP09/10 methodology with the AP09/09 [2], Brazzel and Henderson [7], and the experiment [15,16]. The case considered has a boat-tail angle of 2.93 deg and data were taken at $M_\infty = 1.5$ and 2.5 with $M_j = 2.7$ and $d_j/d_r = 0.45$. Note the AP09/10 shows improvement over the AP09/09. Of course the Brazzel method again significantly underpredicts the base pressure at higher values of C_T due to no control on (T_j/T_j^*) and constant values of $C_1 = 0.19$ and $C_2 = 1.28$ for all values of C_T and M_∞.

Equation (10) shows that, for flares, Eq. (13) is used directly for values of C_T less than 25 with $f(d_B/d_r)$ going to 1 for $C_T \ge 75.0$. Several refinements were made to this methodology. However, these refinements were based on data [17] for Mach numbers from 0.7 to 1.2, as these were the only power-on base pressure data the authors could find for flare cases. As a result, further refinement of the power-on base drag methodology for flares may be possible if additional data at higher Mach numbers becomes available. The equation used for the flare is

$$f(d_B/d_r) = 1 + [(C_T)_e - C_T][f(d_B/d_r)_1 - 1]/[(C_T)_e - 10] \tag{16}$$

where $f(d_B/d_r)_1$ is defined by Eq. (13), and $(C_T)_e = 200 - 133.3M_\infty$, $M_\infty < 1.2 = 200$: $M_\infty < 0.7 = 40$, $M_\infty \le 1.2$, and $f(d_B/d_r) = 1$ for $C_T \le 40$.

New Methodology to Predict Base Pressure Below Values of C_T at which the Minimum Value of P_B/P_∞ Occurs

To define values of P_B/P_∞ for various values of RMF or thrust coefficients between points B and C in Fig. 1 requires two things. First, a definition of point B from the base bleed methodology of [4] is required. Second, a definition of point C where the minimum value of P_B/P_∞ occurs is needed. Knowing points B and C will allow an approximation of the value of P_B/P_∞ for values of RMF between points B and C.

Point B was defined in [4] by the relationship

$$(I_{\max})_{\text{cold}} = .0331\left(\frac{d_j}{d_r}\right)^2 + .0118\left(\frac{d_j}{d_r}\right) \tag{17}$$

$$(I_{\max})_{\text{hot}} \cong 2/3(I_{\max})_{\text{cold}} \tag{18}$$

and $I_{\max} \le 0.025$, where $I_{\max}$ is the maximum value of the base bleed injection parameter at which accurate values of P_B/P_∞ can be predicted from the base bleed methodology of [4].

The base bleed injection parameter was used by Danberg [6] to define base drag. The injection parameter I is defined by the mass rate of flow out of the jet to the mass rate of flow of the freestream with area equal to that of the body cross section, that is,

$$I \equiv \frac{\dot{m}_j}{\dot{m}_\infty} = \frac{\rho_j A_j V_j}{\rho_\infty A_r V_\infty} \tag{19}$$

On the other hand, the jet momentum flux ratio parameter is defined by the momentum out of the jet to that of the freestream of an area equal to the body cross section, that is,

$$\text{RMF} \equiv \frac{\gamma_j P_j d_j^2 M_j^2}{\gamma_\infty P_\infty d_r^2 M_\infty^2} = \frac{(\dot{m}V)_j}{(\dot{m}V)_\infty} \tag{20}$$

Thus,

$$\text{RMF} = I(V_j/V_\infty) \tag{21A}$$

$$(\text{RMF})_B = (I_{\max})(V_j/V_\infty) \tag{21B}$$

Unfortunately, V_j is generally not known for base bleed. It is known that V_j is generally not too large to maintain a longer burn time with a small amount of propellant and, hence, to optimize range. We will therefore assume that $V_j/V_\infty = 0.2$ so that

$$(\text{RMF})_B = I_{\max}/5 \tag{21C}$$

This means that if we have an upper value of 0.025 for $I_{\max}$ where P_B/P_∞ is a maximum (point B on Fig. 1), this value is 0.005 when translated to the P_B/P_∞ versus RMF curves of Fig. 1. Also, C_T is related to RMF through Eq. (1).

Danberg [6] defines the base pressure of region AB in Fig. 1 by

$$P_B/P_\infty = (P_B/P_\infty)_{I=0} + \frac{\sigma I}{1 + \beta\sigma I} \tag{22A}$$

where

$$\sigma = (-5.395 + .0172T_j)M_\infty + (4.61 - .0146T_j)M_\infty^2 + [-.566 + .00446T_j]M_\infty^3 \tag{22B}$$

$$\beta = 15.1\text{–}46.3(M_\infty - 0.71) \tag{22C}$$

$$(P_B/P_\infty)_{I=0} = \frac{\gamma_\infty M_\infty^2}{2} C_{P_B} + 1 \tag{22D}$$

C_{P_B} in Eq. (22D) comes from the power-off values of the AP09 [2]. As already mentioned, I is the mass flow out of the bleed exit to that of the stream tube with area equal to the body cross-sectional area [see Eq. (19)]. Also, because we are interested in the base pressure ratio at point B, we simply substitute $I_{\max}$ into Eq. (22A) to obtain

$$(P_B/P_\infty)_B = (P_B/P_\infty)_{I=0} + \frac{\sigma I_{\max}}{1 + \beta\sigma I_{\max}} \tag{22E}$$

Equations (21C) and (22E) thus define the values of $(P_B/P_\infty)_B$ and $(\text{RMF})_B$.

To define point C in Fig. 1, [3,13] were used. Brazzel and Henderson [3] and Deep et al. [13] give values of P_B/P_∞ versus thrust coefficient, C_T, or RMF for various values of M_∞ for a nozzle flush with the base with $M_j = 2.7$. Of course, C_T is related to RMF [4] by Eq. (1), and P_j/P_∞ can be related to M_j by the basic definition of the jet momentum flux ratio [see Eq. (20)] as

$$\frac{P_j}{P_\infty} = \text{RMF}\left(\frac{\gamma_\infty}{\gamma_j}\right)\left(\frac{d_r}{d_j}\right)^2\left(\frac{M_\infty}{M_j}\right)^2 \tag{23}$$

Combining Eqs. (1) and (23), one obtains RMF in terms of C_T as

$$\text{RMF} = \frac{\frac{C_T}{2} + \left(\frac{d_j}{d_r}\right)^2 \frac{1}{\gamma_\infty M_\infty^2}}{1 + \frac{1}{\gamma_j M_j^2}} \tag{24}$$

Some references make the approximation that

$$\text{RMF} \approx \frac{C_T}{2} \tag{25}$$

However, the APC used Eq. (1) for the definition of RMF. Thus, using [3,13] and Eqs. (1), (17), and (18), one can define P_B/P_∞ versus RMF for various Mach numbers.

The values of RMF [3,13] at $(P_B/P_\infty)_{\min}$ as a function of Mach number are then obtained and plotted in Fig. 6. Figure 6 extrapolates outside where experimental data are available ($M_\infty < 0.7$ and $M_\infty > 2.5$) so that a complete definition of RMF at $(P_B/P_\infty)_{\min}$ as a function of Mach number can be obtained. As additional experimental data become available at lower or higher Mach numbers, the extrapolated values of RMF can be defined. An equation that approximates the Fig. 6 curve for $M_j = 2.7$ and higher is

$$\begin{aligned}
&(\text{RMF})_C = 6 - 0.6374M_\infty - 14.5675M_\infty^2 + 15.223M_\infty^3 \\
&\quad - 5.7564M_\infty^4 + 0.7502M_\infty^5,\ 0 \le M_\infty \le 2; \\
&(\text{RMF})_C = 0.354 - 0.108M_\infty,\ 2 < M_\infty \le 3.2; \\
&(\text{RMF})_C = 0.01,\ M_\infty > 3.2
\end{aligned} \tag{26}$$

Also notice in Fig. 6 that, for $M_\infty > 1.1$, a separate curve is shown for $M_j = 1.0$, which is approximated based on [13]. The equation for $M_j = 1.0$ is thus

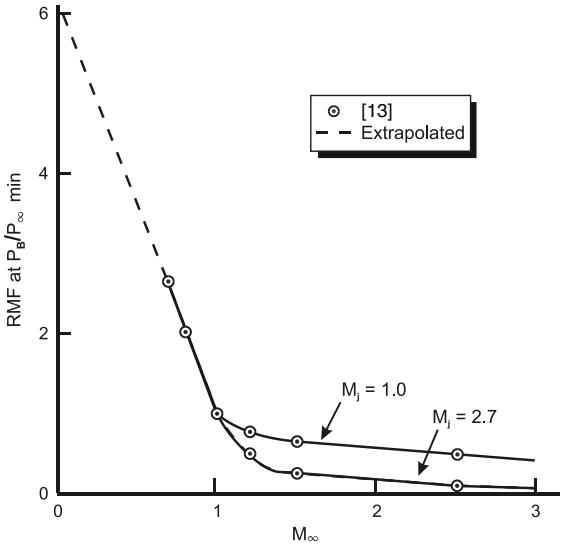

Fig. 6 Jet momentum flux ratio at the point at which P_B/P_∞ is minimum.

$$\begin{aligned}
&(\text{RMF})_C = -0.158M_\infty + 0.775,\ M_\infty > 1.1; \\
&(\text{RMF})_C = 0.01,\ M_\infty > 4.8
\end{aligned} \tag{27}$$

Equation (26) governs the behavior of $(\text{RMF})_C$ for all values of M_j when $M_\infty \le 1.1$. For values of $(\text{RMF})_C$ in between $M_j \ge 2.7$ and 1.0 when $M_\infty > 1.1$, interpolation between the curves in Fig. 6 is used. The value of P_B/P_∞ at point C is then computed using Eq. (5).

Equation (22E) thus defines the value of P_B/P_∞ at point B in Fig. 1. Equation (5), in conjunction with Eqs. (14–16), (26), and (27), define P_B/P_∞ at point C in Fig. 1. Thus, for points in between B and C in Fig. 1, P_B/P_∞ is defined by

$$\begin{aligned}
(P_B/P_\infty)_{BC} = (P_B/P_\infty)_B + (\text{RMF} \\
- (\text{RMF})_B)\left[\frac{(P_B/P_\infty)_C - (P_B/P_\infty)_B}{(\text{RMF})_C - (\text{RMF})_B}\right]
\end{aligned} \tag{28}$$

Equation (28) can be related to C_T through Eq. (1), where

$$\text{RMF} = \left[C_T - \left(\frac{d_j}{d_r}\right)^2 \frac{2}{\gamma_\infty M_\infty^2}\left(\frac{P_j}{P_\infty} - 1\right)\right] \Big/ 2 \tag{29}$$

The new approach (that replaces the modified Brazzel method of the AP09/09 methodology) to compute power-on base drag in the APC is therefore as follows.

If the user of the APC inputs parameters for rocket engine on, the following steps are taken:

1) Compute the lower limit of applicability of the modified Brazzel method using Eqs. (26) and (27).

2) Check to see if RMF $\ge (\text{RMF})_C$. If so, use either the modified Brazzel, Brazzel, or conceptual design method to compute P_B/P_∞.

3) If RMF $< (\text{RMF})_C$, compute values of point B using Eq. (22E), values of point C using Eqs. (5), (26), and (27), and the value of P_B/P_∞ for a given value of RMF using Eq. (28).

If the user of the APC requests either base bleed or power off, no change from the current computational approach of the AP09 will take place.

Results and Discussion

Most of the experimental data used in the validation of the improved power-on base drag prediction model came from [15], which is simply an assessment of several power-on base drag prediction schemes available at the time of publication. The current author received a copy of [15] indirectly from A.L. Addy of the University of Illinois over 25 years ago. As a result, the references used in [15] are shown in Figs. 3–14 so that the reader will be able to access the data if desired. Figures 3 and 4, with data taken from [13,14], have already shown significant improvements in the new power-on base pressure prediction model (AP09/10) for high values of thrust coefficient compared with both the AP09/09 modified Brazzel and the Brazzel methods [7]. Both [13,14] were published after [15] was completed.

Figures 7 and 8 provide additional comparisons of the AP09/10 and AP09/09 with the experimental data [15,16]. Figure 7 shows data for a cylindrical afterbody case, and Fig. 8 shows data for a boat-tail case. Note that the improved AP09/10 of Fig. 7 shows better agreement at all Mach numbers compared with the data than does the January 2009 release (AP09/09) of the aeroprediction code. Figure 8 compares the AP09/10 with the experimental data [18] for several boat-tail cases at $M_\infty = 1.91$ for low values of C_T. Note that the new theory does a good job of predicting where the minimum value of base pressure occurs, but the predicted magnitude of the minimum base pressure is slightly too high. No values of P_B/P_∞ are shown in Fig. 8 for the AP09/09 because the code is not applicable to the low values of C_T.

Figure 9, with experimental data from [15,17], shows data for a low thrust coefficient case. Because values of C_T are all below 1, the

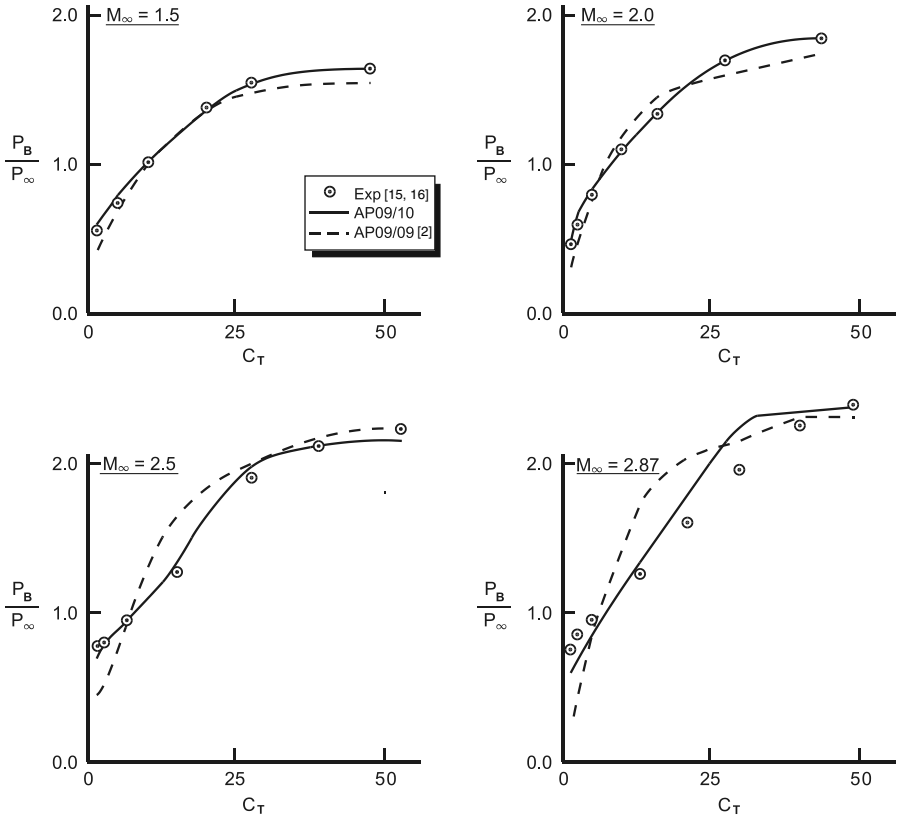

Fig. 7 Comparison of theory and experiment for power-on base pressure prediction ($d_j/d_r = 0.8, d_B/d_r = 1.0, M_j = 2.7$).

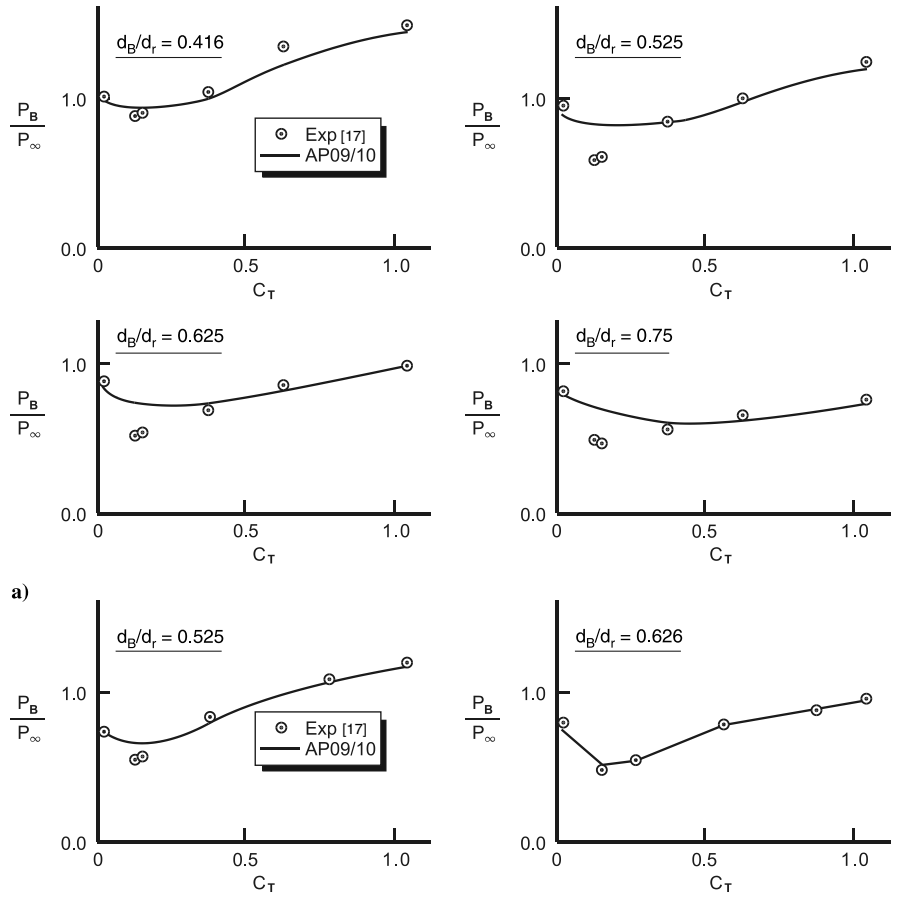

Fig. 8 Comparison of theory and experiment for power-on base pressure: a) $d_j/d_r = 0.375$, $M_\infty = 1.91$, and $M_j = 1.0$; and b) $d_j/d_r = 0.375$, $M_\infty = 1.91$, and $M_j = 2.19$.

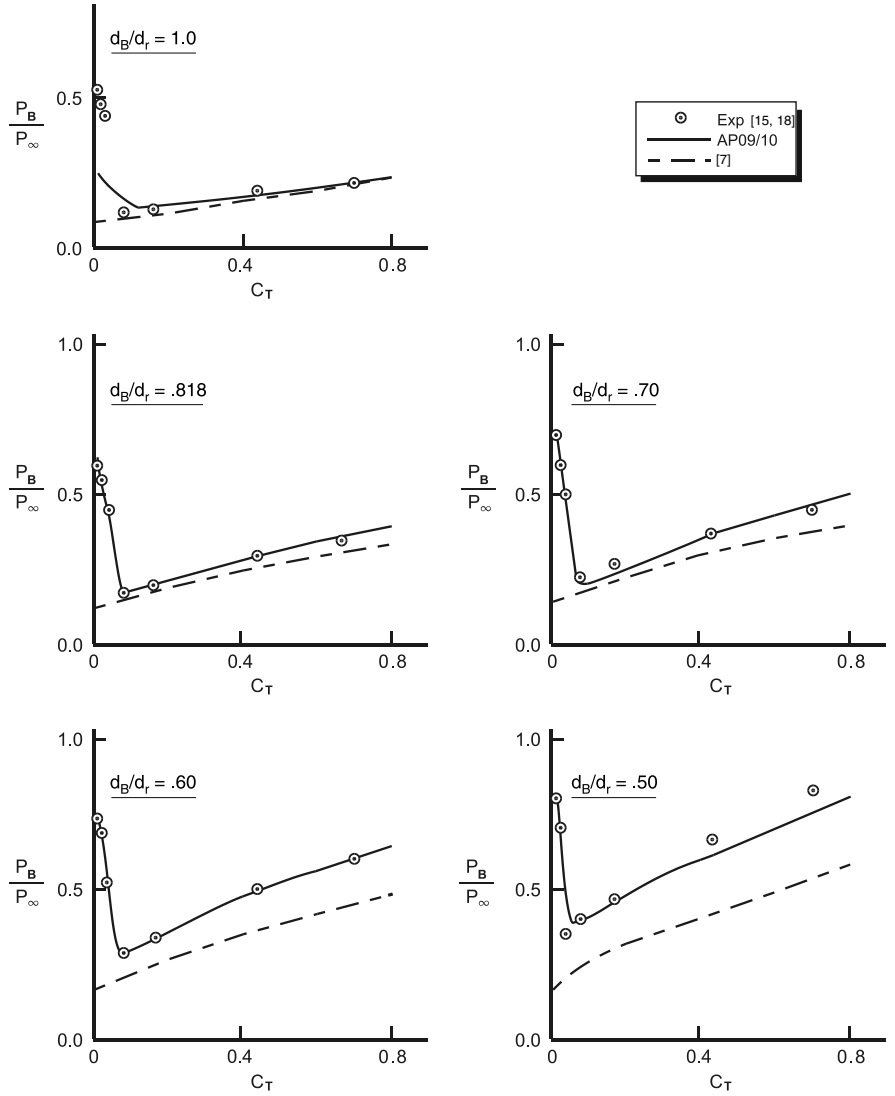

Fig. 9 Comparison of theory and experiment for power-on base pressure ($d_j/d_r = 0.2, M_\infty = 2.5, M_j = 2.7$) for boat-tailed afterbody cases.

AP09/09 values are not shown in this set of curves. However, the Brazzel method, which is actually better at the lower values of C_T than at the higher values of C_T, is shown. Figure 9 consists of five cases, all with $M_\infty = 2.5$, $d_j/d_r = 0.2$, and $M_j = 2.7$. The five cases vary the body base diameter from $d_B/d_r = 0.5$ to 1.0 in increments. All five cases reach the P_B/P_∞ minimum for low values of C_T around 0.08. Note the AP09/10 does a fair job of predicting the minimum value of P_B/P_∞ as well as the increase in P_B/P_∞ after the minimum is reached.

Figure 10 shows the power-on base pressure for a cylindrical afterbody case at $M_\infty = 1.94$ and $M_j = 2.5$ and 3.5. The AP09/10 again shows improvement in comparison with the experimental data given in [15] (which was taken from [19]) compared with the AP09/09. Figure 11 shows additional comparisons of the theory with the experimental data [15,19]. In the cylindrical afterbody case considered, $d_j/d_r = 0.5$, $M_\infty = 2.41$ and $M_j = 1.0$. Data indicate the minimum value of P_B/P_∞ is reached, and the AP09/10 shows good agreement with data before and after $(P_B/P_\infty)_{\min}$ is reached.

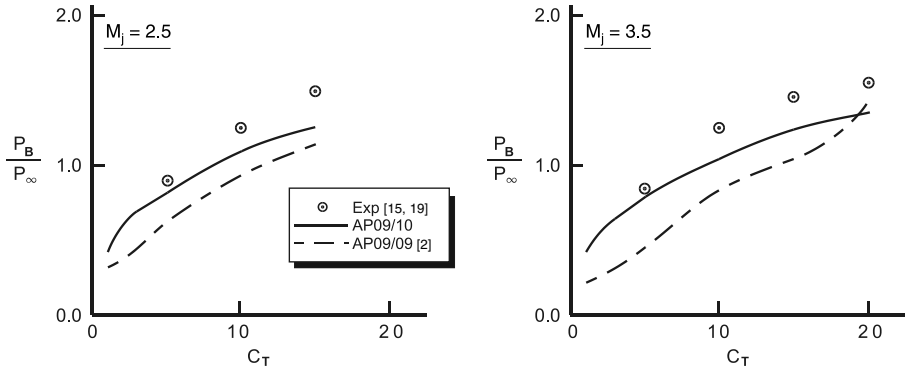

Fig. 10 Comparison of theory and experiment for power-on base drag ($d_j/d_r = .75, d_B/d_r = 1.0, M_j = 1.94$).

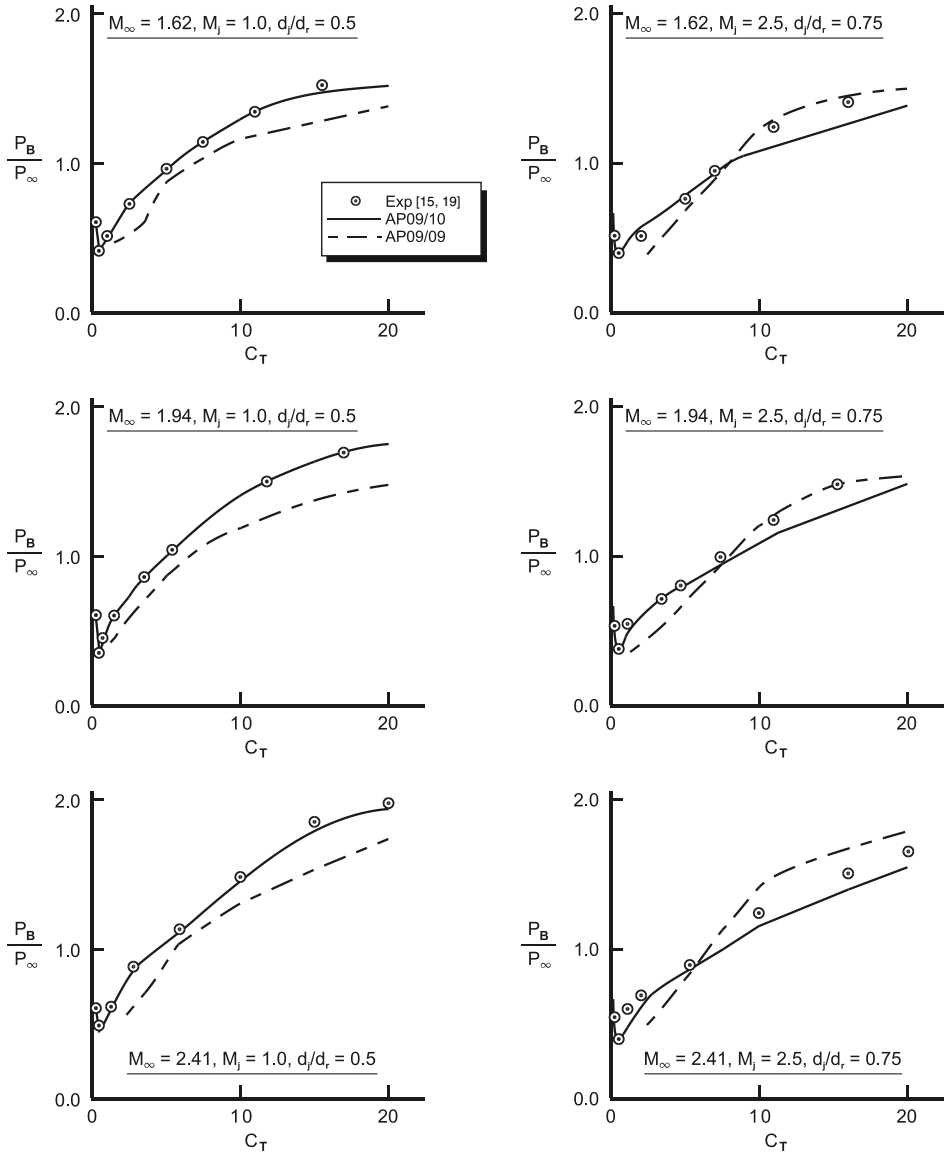

Fig. 11 Comparison of theory and experiment for power-on base pressure ($d_B/d_r = 1.0$).

The next two cases are for cylindrical afterbodies. Figure 12 is for a Mach number of 1.97 and Fig. 13 is for a Mach number of 2.5. Both these cases are for low thrust coefficients. The theory predicts the minimum value of P_B/P_4 to occur at a C_T of about 0.38 at Mach 1.97, whereas the data do not show the minimum to occur at this high a value of C_T. Otherwise, a comparison of the AP09/10 predictions to the data in [15,19] is excellent. For the Mach 2.5 case in Fig. 13, the data suggest a minimum value of P_B/P_∞ occurs at a C_T of about 0.12

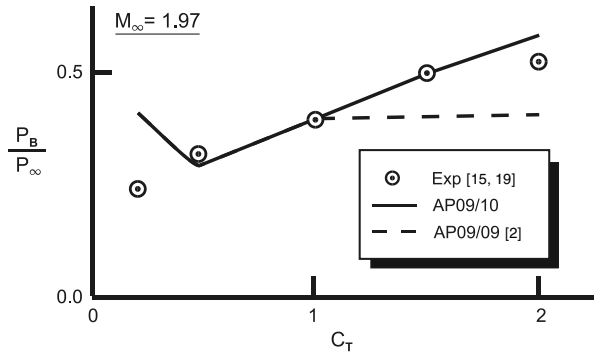

Fig. 12 Comparison of theory and experiment for power-on base pressure ($d_j/d_r = 0.25, d_B/d_r = 1.0, M_j = 1.78$).

and the theory does a good job in predicting all values of base pressure.

The final case (see Fig. 14) considered is the Mach 2.0 cylindrical afterbody example [15,20]. The jet exit Mach number is also 2.0 and $d_j/d_r = 0.6$. Low values of thrust coefficient are available here, and the minimum value of P_B/P_∞ is reached at $C_T = 0.2$ experimentally and at approximately 0.3 theoretically. The theory is slightly higher than the data at $C_T = 3.0$ but is in reasonably good agreement with the data for values of C_T less than about 1.5.

It should be pointed out that, in neither the Brazzel method nor the AP09/09 or AP09/10 methods, is the jet exit angle θ_j considered a variable. However, some data [16] show a strong dependence of P_B/P_∞ on θ_j, whereas other data [14] show little dependence of θ_j values from 9 to 23 deg on P_B/P_∞. The key consideration, it appears, is whether the jet exit angle approaches zero such as would occur on a contoured plume. A contoured plume requires the flow to be turned from an expansion in the nozzle back to a compression to get a value of $\theta_j = 0$ (except for a sonic nozzle, for which no expansion exists). From a practical standpoint, a contoured nozzle requires extra body length of about a caliber or so and extra weight. Many program managers are not willing to sacrifice this extra length and weight to allow for a contoured nozzle. Hence, it is believed that, for most rocket nozzles, the new AP09/10 methodology will give reasonably accurate values of P_B/P_∞ even though θ_j is not explicitly included in the formulation.

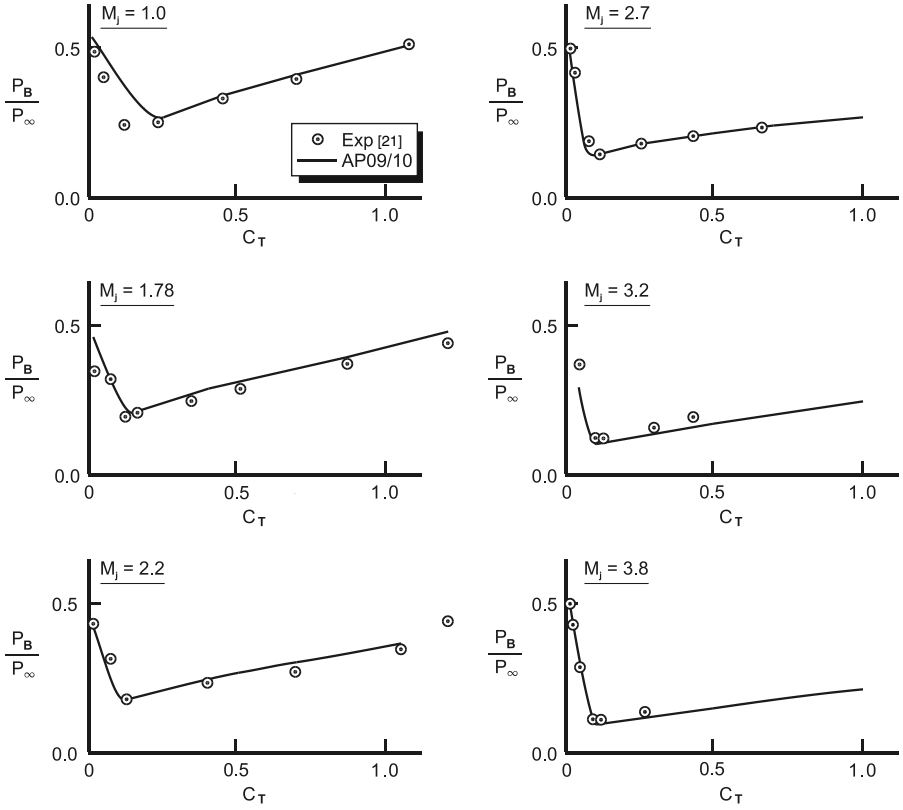

Fig. 13 Comparison of theory and experiment for power-on base pressure ($d_j/d_r = 0.2 d_B/d_r = 1.0, M_\infty = 2.5$).

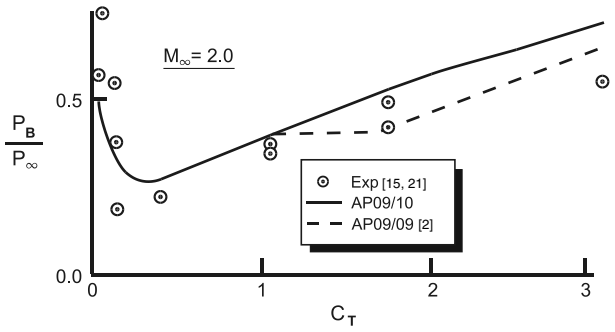

Fig. 14 Comparison of theory and experiment for power-on base pressure ($d_j/d_r = 0.6, d_B/d_r = 1.0, M_j = 2.0$).

Conclusions

To summarize, the modified Brazzel method to predict the power-on base pressure of the AP09/09 has been improved and will be released in January 2010 as the AP09/10. Improvements to the AP09/09 include modifications to the constants $C_1(M_\infty, C_T)$ and $C_2(M_\infty, C_T)$ and to the terms (T_j/T_j^*) and $f(d_B/d_r)$. In addition, a new method was developed to predict the base pressure below the point at which the minimum base pressure occurs. A comparison of the new theory with the experiment and the AP09/09 and Brazzel methods indicated significant improvements in accuracy for the AP09/10 for most cases considered. Power-on base pressure and base pressure drag can now be computed over the entire range of thrust coefficients from power off to very high values typical of a booster rocket.

References

[1] Moore, F. G., and Hymer, T. C., "The 2005 Version of the Aeroprediction Code: Part I—Summary of the New Methodology," Aeroprediction, Inc., Rept. 1, Jan. 2004.

[2] Moore, F. G., and Moore, L. Y., "The 2009 Version of the Aeroprediction Code: The AP09," Aeroprediction, Inc., Rept. 3, Jan. 2008.

[3] Brazzel, C. E., and Henderson, J. H., "Effects of Sustainer Rocket Nozzle Diameter and Location of the Power-on Base Pressure of a Body of Revolution with Concentric Boost and Sustainer Rocket Nozzles at Transonic Speeds," U. S. Army Missile Command, Rept. RD-TR-67-11, Redstone Arsenal, AL, Oct. 1967.

[4] Brazzel, C. E., "The Effects of Base Bleed and Sustainer Rocket Nozzle Diameter and Location on the Base Drag of a Body of Revolution with Concentric Boost and Sustainer Rocket Nozzles," U. S. Army Missile Command, Rept. RD-TR-63-23, Redstone Arsenal, AL, July 1963.

[5] Moore, F. G., and Hymer, T. C., "The 2002 Version of the Aeroprediction Code: Part I—Summary of New Theoretical Methodology," Naval Surface Warfare Center Dahlgren Division Rept. TR-01/108, March 2002.

[6] Danberg, J. E., "Analysis of the Flight Performance of the 155MM M864 Base Burn Projectile," Army Research Laboratory, Rept. BRL-TR-3083, Aberdeen, MD, April 1990.

[7] Brazzel, C. E., and Henderson, J. H., "An Empirical Technique for Estimating Power-On Base Drag of Bodies-of-Revolution with a Single Jet Exhaust," *The Fluid Dynamics Aspects of Ballistics*, CP10, NATO-AGARD, Paris, pp. 241–61, Sept. 1966.

[8] Moore, F. G., "Body Alone Aerodynamics of Guided and Unguided Projectiles at Subsonic, Transonic, and Supersonic Mach Numbers," Naval Weapons Lab., Rept. NWL-TR-2976, Dahlgren, VA, Nov. 1972.

[9] Moore, F. G., "Aerodynamics of Guided and Unguided Weapons: Part I—Theory and Application," Naval Weapons Lab., Rept. NWL TR-3018, Dahlgren, VA, Dec. 1973.

[10] Moore, F. G., and Swanson, R. C., "Aerodynamics of Tactical Weapons to Mach Number 3 and Angle of Attack 15 Degrees: Part I—Theory and Application," Naval Surface Warfare Center Dahlgren Laboratory TR-3584, Dahlgren, VA, Feb. 1977.

[11] Moore, F. G., Hymer, T. C., and McInville, R. M., "Improved Aeroprediction Code: Part I—Summary of New Methods and Comparison with Experiment," Naval Surface Warfare Center Dahlgren Division, TR-93/91, May 1993.

[12] Moore, F. G., Wilcox, F. J., and Hymer, T. C., "Improved Empirical Model for Base Drag Prediction on Missile Configurations Based on New Wind Tunnel Data," Naval Surface Warfare Center Dahlgren Division, TR-92/509, Oct. 1992.

[13] Deep, R. A., Henderson, J. H., and Brazzel, C. E., "Thrust Effects on Missile Aerodynamics," U.S. Army Missile Command, Rept. RD-TR-71-9, Redstone Arsenal, AL, May 1971.

[14] Henderson, J. H., "An Investigation for Modeling Jet Plume Effects on Missile Aerodynamics," U. S. Army Missile Command, TR RD-CR-82-25, July 1982.
[15] King, H. A., "An Assessment of a Method Developed by U. S. Army Missile Command for Predicting Base Pressure of a Body of Revolution with a Hot Jet Efflux," British Aircraft Corp., Rept. ST 14691, Bristol, England, U.K., March 1976.
[16] Craft, J. C., and Brazzel, C. E., "An Experimental Investigation of Base Pressure on a Body of Revolution at High Thrust Levels and Free Steam Mach Numbers of 1.5 to 2.87," U. S. Army Missile Command Report No. RD-TM-70-6, Redstone Arsenal, AL, July 1970.
[17] Bromm, A. F., and O'Donnell, R. M., "Investigation at Supersonic Speeds of the Effect of Jet Mach Number and Divergence Angle of the Nozzle Upon the Pressure of the Base Annulus of a Body of Revolution," NACA RM L54I16, Dec. 1954.
[18] Rubin, D. V., Brazzel, C. E., and Henderson, J. H., "The Effects of Jet Plume and Boattail Geometry on Base and Afterbody Pressures of a Body of Revolution at Mach Numbers of 2.0 to 3.5," U. S. Army Missile Command Rept. RD-TR-70-5, April 1970.
[19] Lilienthal, P. F., Brink, D. F., and Addy, A. L., "Experimental Program for the Study of Supersonic and Transonic Axisymmetric Base Pressure Problems," Univ. of Illinois, July 1970.
[20] Reid, J., and Hastings, R. C., "The Effect of Central Jet on the Base Pressure of a Cylindrical Afterbody in Supersonic Stream," Royal Aircraft Establishment Rept. Aero 2621, Farnborough, England, U.K., Dec. 1959.
[21] Martin, T. A., and Brazzel, C. E., "Investigation of the Effect of Low Thrust Levels on the Base Pressure of a Cylindrical Body at Supersonic Speeds," U.S. Army Materiel Command, RD-TR-70-11, Redstone Arsenal, AL, May 1970.

J. Martin
Associate Editor